29th International Conference
ENGINEERING MECHANICS 2023
Milovy, Czech Republic, May 9 – 11, 2023

DYNAMICS OF A CANTILEVER BEAM WITH PIEZOELECTRIC SENSOR: FINITE ELEMENT MODELING

Cimrman R.*, Kolman R., Musil L.***, Kotek V.†, Kylar J.‡**

Abstract: *An elastodynamical model of a cantilever beam coupled with a piezoelectric sensor is introduced and its discretization using the finite element method is presented. The mathematical model includes additional terms that enforce the floating potential boundary condition for keeping a constant charge on an electrode of the sensor. The behaviour of the model is illustrated using a numerical example corresponding to an experimental setup, where vibrations of the beam and the potential on the sensor are measured.*

Keywords: Finite element method, Piezo-electricity, Floating potential, Dynamic simulation.

1. Introduction

In this contribution we describe a theoretical elastodynamical model of a cantilever beam with an attached piezoelectric sensor. The setup models the experiments reported in (Kolman et al., 2023) in these proceedings. The work represents our initial step in research towards employing the piezoelectric and flexoelectric effects for energy harvesting (Hamlehdar et al., 2019) and related investigation of acoustic/dynamical properties of periodic 3D printed active meta-materials — we have deliberately used a simple experiment to calibrate our measuring equipment and modelling tools.

The finite element (FE) (Zienkiewicz et al., 2013) model is defined in terms of the stress–electric displacement formulation of piezoelectricity (Yang, 2018). The floating potential boundary condition is applied to model the voltage measurement using a voltmeter with a large internal resistance – this condition introduces an additional unknown to the model. Illustrative results of a numerical calculation are presented.

2. The Finite Element Model

The model presented below corresponds to our experimental setup (Kolman et al., 2023), where a cantilever beam is firmly attached on one end and statically deformed by a weight hanging on a thin nylon string from the other end. The weight is then suddenly removed by cutting the string and the beam vibrations in a selected point and the voltage generated on the sensor piezoelectric sensor glued to the beam are recorded.

Let us consider a body with domain $\Omega \subset \mathbb{R}^3$ consisting of an elastic part Ω_E and a piezoelectric part Ω_P. In our setting, the elastic part is the cantilever beam fixed on its side Γ_u, and the piezoelectric part is the cylindrical sensor attached to the beam as shown in Fig. 1. Under linear assumptions, the constitutive relations of the piezoelastic solid in Ω_P can be written as

$$\boldsymbol{\sigma} = \boldsymbol{C}^P\boldsymbol{\varepsilon} - \boldsymbol{e}^T\boldsymbol{E}\,, \quad \boldsymbol{d} = \boldsymbol{e}\boldsymbol{\varepsilon} + \boldsymbol{\kappa}\boldsymbol{E}\,, \quad \boldsymbol{\varepsilon} = \frac{1}{2}(\boldsymbol{\nabla}\boldsymbol{u} + \boldsymbol{\nabla}^T\boldsymbol{u})\,, \quad \boldsymbol{E} = -\boldsymbol{\nabla}\varphi\,, \tag{1}$$

where the mechanical stress $\boldsymbol{\sigma}$ (in Voigt notation vector ordering) and the electric displacement $\boldsymbol{d}$ are proportional to the mechanical strain $\boldsymbol{\varepsilon}$ and the electric field vector $\boldsymbol{E}$, $\boldsymbol{u}$ is the mechanical displacement

* Robert Cimrman, Institute of Thermomechanics of the CAS, Prague & New Technologies - Research Centre and Faculty of Applied Sciences, University of West Bohemia, Plzeň; CZ, cimrman3@ntc.zcu.cz
** Radek Kolman, Institute of Thermomechanics of the CAS, Prague & College of Polytechnics Jihlava; CZ, kolman@it.cas.cz
*** Ladislav Musil, Institute of Thermomechanics of the CAS, Prague; CZ, musill@it.cas.cz
† Vojtěch Kotek, Institute of Thermomechanics of the CAS, Prague; CZ, kotek@it.cas.cz
‡ Jaromír Kylar, Institute of Thermomechanics of the CAS, Prague; CZ, kylar@it.cas.cz

ISSN: 1805-8256, doi: 10.21495/em2023-51

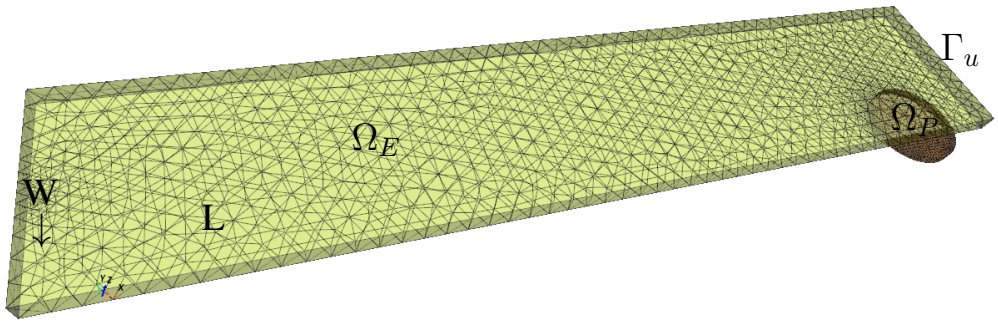

Fig. 1: The computational domain with the FE mesh. A static weight is attached to the bottom side at the point W at time $t = 0$ s. Dynamic motion quantities are recorded in the point L, corresponding to the point of laser vibrometer measurements in the related experiments.

vector, φ the electric potential, $\boldsymbol{C}^P$ the matrix of elastic properties under constant electric field intensity, $\boldsymbol{e}$ the piezoelectric modulus and $\boldsymbol{\kappa}$ the permittivity under constant deformation. In Ω_E we have simply $\boldsymbol{\sigma} = \boldsymbol{C}^E\boldsymbol{\varepsilon}$. The strong form of our piezo-elastodynamics problem to be solved in time $t \in [0, T]$ is: Find $\boldsymbol{u}$, φ, $\bar{\varphi}(t)$ such that

$$\begin{aligned}
\rho\ddot{\boldsymbol{u}} - \boldsymbol{\nabla}\cdot\boldsymbol{\sigma} &= \boldsymbol{b} \text{ in } \Omega\times[0,T]\,,\\
\boldsymbol{\nabla}\cdot\boldsymbol{d} &= 0 \text{ in } \Omega_P\times[0,T]\,,\\
\boldsymbol{u} &= 0 \text{ on } \Gamma_u\times[0,T]\,,\\
\varphi &= 0 \text{ on } \Gamma_{p0}\times[0,T]\,,\\
\varphi &= \bar{\varphi}(t) \text{ on } \Gamma_{pQ}\times[0,T] \text{ such that } \int_{\Gamma_{pQ}}(\boldsymbol{\kappa}\boldsymbol{\nabla}\varphi)\cdot\boldsymbol{n} = Q\,,\\
\boldsymbol{u}|_{t=0} = \boldsymbol{u}^0\,,&\quad \dot{\boldsymbol{u}}|_{t=0} = \dot{\boldsymbol{u}}^0\,,\quad \varphi|_{t=0} = \varphi^0 \text{ in } \Omega\,,
\end{aligned} \tag{2}$$

where ρ is the material density and $\boldsymbol{b}$ are the self-weight volume forces. Zero potential is prescribed on Γ_{p0}, the bottom side of the piezo-sensor that is attached to the beam. The scalar $\bar{\varphi}(t)$ on the top side of the sensor Γ_{pQ} is an additional unknown variable, so called *floating potential*, that evolves in time so that the initial charge Q on Γ_{pQ} is conserved. Zero Neumann boundary conditions are applied on the parts of $\partial\Omega$ not mentioned above. The initial charge is determined from the initial state $\boldsymbol{u}^0$, $\dot{\boldsymbol{u}}^0$ and φ^0 corresponding to a static loading of the body by a localized surface force of a weight attached at point W in Fig. 1.

Let $V_0^u(\Omega) = \{\boldsymbol{u}\in[H^1(\Omega)]^3, \boldsymbol{u} = \boldsymbol{0} \text{ on } \Gamma_u\}$, $V_0^\varphi = \{\varphi\in H^1(\Omega), \varphi = 0 \text{ on } \Gamma_{p0}\}$. The weak form of (2) is then: Find $\boldsymbol{u}$, φ, $\bar{\varphi}(t)$ such that

$$\int_\Omega \rho\boldsymbol{v}\cdot\ddot{\boldsymbol{u}} + \int_\Omega \boldsymbol{\varepsilon}(\boldsymbol{v})^T\boldsymbol{C}\boldsymbol{\varepsilon}(\boldsymbol{u}) - \int_{\Omega_P}\boldsymbol{\varepsilon}(\boldsymbol{v})^T\boldsymbol{e}^T\boldsymbol{\nabla}\varphi - \int_\Omega \boldsymbol{v}\cdot\boldsymbol{b} = 0 \quad \forall\boldsymbol{v}\in V_0^u(\Omega)\,, \tag{3}$$

$$\int_{\Omega_P}(\boldsymbol{\nabla}\psi)^T\boldsymbol{e}\boldsymbol{\varepsilon}(\boldsymbol{u}) + \int_{\Omega_P}(\boldsymbol{\nabla}\psi)^T\boldsymbol{\kappa}\boldsymbol{\nabla}\varphi - \int_{\Gamma_{pQ}}(\boldsymbol{\kappa}\boldsymbol{\nabla}\varphi)\cdot\boldsymbol{n}\psi + \int_{\Gamma_{pQ}}(\boldsymbol{\kappa}\boldsymbol{\nabla}\psi)\cdot\boldsymbol{n}(\varphi-\bar{\varphi}) = 0 \quad \forall\psi\in V_0^\varphi(\Omega)\,, \tag{4}$$

$$\int_{\Gamma_{pQ}}(\boldsymbol{\kappa}\boldsymbol{\nabla}\varphi)\cdot\boldsymbol{n} - Q = 0\,, \tag{5}$$

where (5) expresses the floating potential condition and the last two terms in (4) correspond to the weak enforcement of the Dirichlet boundary condition $\varphi = \bar{\varphi}(t)$ on Γ_{pQ} using the non-symmetric Nitsche's method (Nitsche, 1971) without the penalty term (Burman, 2012).

The FE discretization of the model uses the approximations

$$\boldsymbol{u}(\boldsymbol{\xi}) = \mathbf{N}_u(\boldsymbol{\xi})\mathbf{u}\,,\quad \varphi(\boldsymbol{\xi}) = \mathbf{N}_\varphi(\boldsymbol{\xi})\mathbf{p}\,,\quad \bar{\varphi} = 1\bar{p}\,, \tag{6}$$

where $\mathbf{N}_u(\boldsymbol{\xi})$, $\mathbf{N}_\varphi(\boldsymbol{\xi})$ are the shape functions for the discretization of the displacements and the potential, respectively. Substituting (6) into (3)–(5) yields the following semi-discrete equations:

$$\begin{bmatrix}\mathbf{M} & \mathbf{0} & \mathbf{0}\\ \mathbf{0} & \mathbf{0} & \mathbf{0}\\ \mathbf{0} & \mathbf{0} & 0\end{bmatrix}\begin{bmatrix}\ddot{\mathbf{u}}\\ \ddot{\mathbf{p}}\\ \ddot{\bar{p}}\end{bmatrix} + \begin{bmatrix}\mathbf{K} & -\mathbf{B}^T & \mathbf{0}\\ \mathbf{B} & \mathbf{C}-\mathbf{F}+\mathbf{F}^T & -\mathbf{F}^T\mathbf{1}\\ \mathbf{0} & \mathbf{1}^T\mathbf{F} & 0\end{bmatrix}\begin{bmatrix}\mathbf{u}\\ \mathbf{p}\\ \bar{p}\end{bmatrix} - \begin{bmatrix}\mathbf{b}\\ \mathbf{0}\\ Q\end{bmatrix} = \mathbf{0}\,, \tag{7}$$

where $\mathbf{M}$ is the mass matrix, $\mathbf{K}$ is the stiffness matrix, $\mathbf{B}$ is the piezoelastic coupling matrix, $\mathbf{C}$ is the electrostatic potential matrix and $\mathbf{b}$ the volume forces vector. The surface flux matrix $\mathbf{F} = \int_{\Gamma_{pQ}} \mathbf{N}_\varphi^T \boldsymbol{n}\boldsymbol{\kappa}\mathbf{N}'_\varphi$ serves to impose weakly the floating potential condition, together with $\mathbf{1}$, the matrix of ones, used to sum the rows of $\mathbf{F}$, performing thus the integration of (5). Because the potentials $\mathbf{p}$, $\bar{p}$ occur in (7) without time derivatives, a time discretization scheme needs to be applied only to $\mathbf{u}$. We use the implicit second order Newmark method (Newmark, 1959) with the standard settings $\beta = \frac{1}{4}$, $\gamma = \frac{1}{2}$, leading to the following linear system solved in every time step n:

$$\begin{bmatrix} \mathbf{M} + \beta\Delta t^2\mathbf{K} & -\mathbf{B}^T & \mathbf{0} \\ \beta\Delta t^2\mathbf{B} & \mathbf{C} - \mathbf{F} + \mathbf{F}^T & -\mathbf{F}^T\mathbf{1} \\ \mathbf{0} & \mathbf{1}^T\mathbf{F} & 0 \end{bmatrix} \begin{bmatrix} \mathbf{a}^n \\ \mathbf{p}^n \\ \bar{p}^n \end{bmatrix} = \begin{bmatrix} \mathbf{b} \\ \mathbf{0} \\ Q \end{bmatrix}, \tag{8}$$

where Δt is the current time increment, $\mathbf{u}^n = \mathbf{u}^{n-1} + \Delta t\mathbf{v}^{n-1} + \Delta t^2((\frac{1}{2} - \beta)\mathbf{a}^{n-1} + \beta\mathbf{a}^n)$, and $\mathbf{v}^n = \mathbf{v}^{n-1} + \Delta t((1-\gamma)\mathbf{a}^{n-1} + \gamma\mathbf{a}^n)$.

3. Numerical Example

To illustrate the behaviour of the model described above we simulate the time evolution of the setup in Fig. 1 for $t = [0, 0.02]$ s with the following material parameters:

- Steel elastic beam: $\rho = 7800$ kg/m^3, $E = 210$ GPa, $\nu = 0.3$.
- Piezoelectric disc: $\rho = 7800$ kg/m^3, the vacuum permittivity $\varepsilon^0 = 8.8541878128 \cdot 10^{-12}$ F/m and

$$\text{in Voigt notation: } \boldsymbol{C}^P = \begin{bmatrix} 127.2050 & 80.2122 & 84.6702 & 0.0000 & 0.0000 & 0.0000 \\ 80.2122 & 127.2050 & 84.6702 & 0.0000 & 0.0000 & 0.0000 \\ 84.6702 & 84.6702 & 117.4360 & 0.0000 & 0.0000 & 0.0000 \\ 0.0000 & 0.0000 & 0.0000 & 22.9885 & 0.0000 & 0.0000 \\ 0.0000 & 0.0000 & 0.0000 & 0.0000 & 22.9885 & 0.0000 \\ 0.0000 & 0.0000 & 0.0000 & 0.0000 & 0.0000 & 23.4742 \end{bmatrix} \text{ GPa,}$$

$$\boldsymbol{e} = \begin{bmatrix} 0.00000 & 0.00000 & 0.0000 & 0.0000 & 17.0345 & 0.0 \\ 0.00000 & 0.00000 & 0.0000 & 17.0345 & 0.0000 & 0.0 \\ -6.62281 & -6.62281 & 23.2403 & 0.0000 & 0.0000 & 0.0 \end{bmatrix} \text{ C/m}^2, \boldsymbol{\kappa} = \varepsilon^0 \begin{bmatrix} 1704.4 & 0.0 & 0.0 \\ 0.0 & 1704.4 & 0.0 \\ 0.0 & 0.0 & 1433.6 \end{bmatrix} \text{ F/m .}$$

All results reported here were obtained using the Open Source finite element software SfePy (Cimrman et al., 2019; Cimrman, 2021). The initial state was a result of a static calculation with the gravity load by 280 g weight attached in the point W. Zero Dirichlet boundary conditions were applied to φ on both sides of the piezoelectric disc, corresponding to a short-circuited state. The initial charge $Q = \int_{\Gamma_{pQ}} (\boldsymbol{\kappa}\boldsymbol{\nabla}\varphi) \cdot \boldsymbol{n}$ was determined to be $-3.06 \cdot 10^{-8}$ C. The transient calculation then proceeded as described in (3)–(5), resp. in (8). Time histories of $\boldsymbol{u}$, $\dot{\boldsymbol{u}}$ and $\ddot{\boldsymbol{u}}$ in the point L were recorded, as well as the charges on the Γ_{pQ} (top) and Γ_{p0} (bottom) disc surfaces and the floating potential $\bar{\varphi}$, which corresponded directly to the measured voltage, see Fig. 2. To verify the time-dependent calculation, we computed the Lomb-Scargle periodogram (Lomb, 1976; Scargle, 1982) of $u_3(t)$ in L (Fig. 2–B). The principal frequency of the signal agrees well with the red vertical line marking the lowest frequency $f_1 = 166.3$ Hz determined by the modal analysis. This value is also consistent with the theoretical frequency 161.1 Hz and the experimental value 159.4 Hz reported in (Kolman et al., 2023) in these proceedings. The effect of the floating potential boundary condition can be seen in Fig. 2–C, where $Q(t)$ on Γ_{pQ} is kept constant.

4. Conclusion

A mathematical model of dynamics of a cantilever beam with a piezoelectric sensor and its FE discretization were presented. A particular treatment of the floating potential boundary condition was shown. The outputs of our custom SfePy-based computer implementation were illustrated using a numerical example, designed to follow the experiments in (Kolman et al., 2023) and to verify the correctness of our implementation. In future, the results will be compared in detail to the experimental data reported in (Kolman et al., 2023) and the model will be fitted to accurately describe each of the measured data sets.

Acknowledgments

This work has been supported by the grant 23-06220S of the Czech Science Foundation within institutional support RVO:61388998.

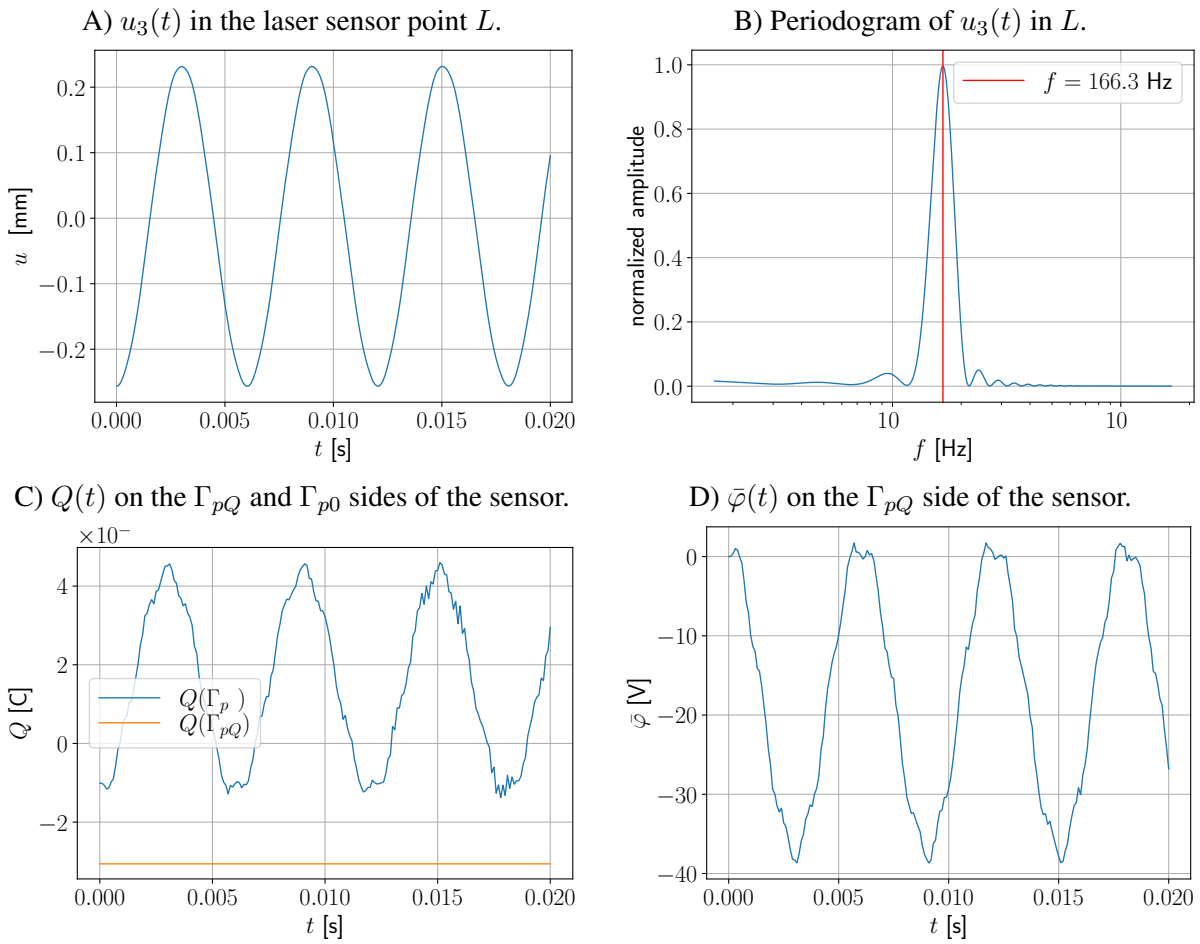

Fig. 2: Time histories of the recorded quantities (A, C, D) and the periodogram (B) of $u_3(t)$ in L with the the vertical red line marking the lowest frequency determined by the modal analysis.

References

Burman, E. (2012) A penalty-free nonsymmetric nitsche-type method for the weak imposition of boundary conditions. *SIAM Journal on Numerical Analysis*, 50, 4, pp. 1959–1981.

Cimrman, R. (2021) Fast evaluation of finite element weak forms using python tensor contraction packages. *Advances in Engineering Software*, 159, pp. 103033.

Cimrman, R., Lukeš, V., and Rohan, E. (2019) Multiscale finite element calculations in python using sfepy. *Advances in Computational Mathematics*, 45, 4, pp. 1897–1921.

Hamlehdar, M., Kasaeian, A., and Safaei, M. R. (2019) Energy harvesting from fluid flow using piezoelectrics: A critical review. *Renewable Energy*, 143, pp. 1826–1838.

Kolman, R., Kylar, J., Kotek, V., Cimrman, R., and Musil, L. (2023) Dynamics of a cantilever beam with piezoelectric sensor: Experimental study. In V. Radolf, I. Zolotarev, edt., *Proceedings of the 29th International Conference Engineering Mechanics 2023, Milovy, May 9-11, 2023*. Institute of Thermomechanics of the Czech Academy of Sciences.

Lomb, N. R. (1976) Least-squares frequency analysis of unequally spaced data. *Astrophysics and Space Science*, 39, 2, pp. 447–462.

Newmark, N. M. (1959) A method of computation for structural dynamics. *Journal of the Engineering Mechanics Division*, 85, 3, pp. 67–94.

Nitsche, J. (1971) Über ein Variationsprinzip zur Lösung von Dirichlet-Problemen bei Verwendung von Teilräumen, die keinen Randbedingungen unterworfen sind. *Abhandlungen aus dem Mathematischen Seminar der Universität Hamburg*, 36, 1, pp. 9–15.

Scargle, J. D. (1982) Studies in astronomical time series analysis. ii. statistical aspects of spectral analysis of unevenly spaced data. *The Astrophysical Journal*, 263, pp. 835–853. ADS Bibcode: 1982ApJ...263..835S.

Yang, J. (2018) *An Introduction to the Theory of Piezoelectricity*, 9 of *Advances in Mechanics and Mathematics*. Springer International Publishing, Cham.

Zienkiewicz, O. C., Taylor, R. L., and Zhu, J. Z. (2013) *The Finite Element Method: Its Basis and Fundamentals*. Butterworth-Heinemann, Oxford.